

Application of Fiber Bragg Grating Sensing Technology in Welding Stress Test

Lijun Meng

School of Electromechanical and Architectural Engineering, Jiang Han University
No.8 Delta Lake Road, Wuhan, Hubei, China
menglijun0408@163.com

Abstract - Welding structures are widely used in various engineering fields. Effective monitoring of stress and temperature during welding process will help to take measures to control the welding deformation. In this paper, the monitoring method of welding stress and temperature based on fiber Bragg grating (FBG) sensor network is presented. First: i) the reliability and effectiveness of the FBG monitoring system in high temperature environment were studied, then ii) the distributed FBG sensing system was used to monitor the online welding stress of the aluminum alloy plates during the butt welding and groove welding processes. The welding stress was detected by the FBG networks in turn according to the welding sequence, and the closer the FBG was to welding seam, the greater the welding stress was. The welding stress caused by groove welding was smaller than that of the butt welding.

Keywords - fiber Bragg grating (FBG); Welding stress; High temperature strain; On line detection.

I. INTRODUCTION

Welding is a process that some locations are heated to high temperature quickly and then cooled fast. In this process, the metal structure has an extremely uneven temperature field, and bears thermal strain and plastic strain, resulting in residual stress[1]. Welding residual stress and deformation are important factors in influencing structural performance, safety and reliability[2-3]. In certain conditions, it will exert a very negative impact on the fracture characteristics, fatigue strength as well as shape and size precision of the structure. Therefore, to study the distribution of welding temperature and stress is useful for taking timely measures to control the welding deformation. FBG has many sensing advantages such as small size, electrical insulation, resistance to electromagnetic interference, high precision and reliability, good environmental adaptability, several measuring gratings in a one fiber to form distributed sensors for different parameters [4]. As a result, it has been widely used in many engineering fields[5-7]. However, the research on the online welding stress monitoring using the optical fiber sensing technology is less. In this paper, the welding stress measurement of the aluminum alloy plate with the pasted FBG was studied.

II. BASIC PRINCIPLE OF FIBER BRAGG GRATING SENSING

When the temperature, strain, or other physical quantity around the grating is changed, the refractive index of the fiber core n or the grating period Λ will be changed, leading to the fluctuation of the Bragg center wavelength λ_B in the reflected wave. The change information of the physical quantity can be obtained by detecting the center wavelength change. The Bragg center wavelength λ_B , the refractive

index of the fiber core n and grating period Λ meet the following relationship:

$$\lambda_B = 2n\Lambda \quad (1)$$

The center wavelength change caused by the temperature and strain $\Delta\lambda_B = \lambda_B - \lambda_{B'}$ can be expressed by the following formula:

$$\Delta\lambda_B = 2n\Lambda \left\{ \left[1 - \frac{n^2}{2} [p_{12} - \nu(p_{11} + p_{12})] \right] \varepsilon + \left[\alpha + \frac{(\frac{dn}{dT})}{n} \right] \Delta T \right\} \quad (2)$$

It can be seen that from Formula (2) that the center wavelength λ_B change with strain ε and temperature T . Therefore, the change of external stress and temperature can be measured by detecting the Bragg center wavelength.

The FBGs around 1310nm band were used in the experiment. The center wavelength varied about 9.54pm when the temperature changed 1°C, that is, the sensitivity of FBG to temperature was 9.54 pm/°C. The center wavelength shifted 1pm with the external strain variation of 1με, and the corresponding strain sensitivity of FBG was 1 pm/με. The relationship between FBG center wavelength and temperature as well as strain was as follows:

$$\frac{\Delta\lambda_B}{\lambda_B} = 1 \times 10^{-6} \mu\varepsilon^{-1} \cdot \varepsilon + 9.54 \times 10^{-6} \cdot ^\circ\text{C} \cdot \Delta T \quad (3)$$

III. INITIAL CALIBRATION OF TEMPERATURE AND STRAIN MEASUREMENT

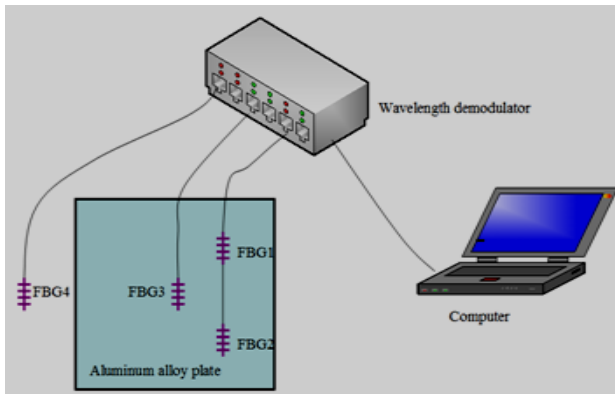


Fig.1 FBG arrangement in temperature and stress calibration experiment.

The temperature is very high during the welding process, therefore it is needed to verify the effectiveness of the FBG signal at a higher temperature to ensure the reliable work of FBG through the welding process.

The layout of measurement FBG sensors was shown in Fig.1. Three pieces of FBG sensor (FBG1,FBG2,FBG3) were pasted on the surface of a square aluminum alloy plate with America UV glue, and the plate was put into the oven after the glue was heating solidification by an electric hair dryer. While, The FBG4 sensor was placed directly in the oven. The temperature in the oven was raised gradually in the following order: 50 °C to 64°C(about 17 minutes), 64°C to 101 °C(about 6 minutes), 114°C to 150°C (about 4 minutes), 164°C to 201 °C (about 3 minutes), 210°C to 250°C (about 4 minutes), 256°C to 300 °C (about 4 minutes), 308°C to 351°C (about 5 minutes) . Record the FBG output data.

Because the temperature changed very slowly, the curves were smoothed by averaging adjacent datum to reduce the data aliasing of different channels and signal distortion caused by temperature rise. And then the Formula (3) was used to separate the external temperature and stress which both influenced the grating center wavelength change. Finally the temperature change in the oven measured by FBG4 and the thermal stress changes at the paste position of FBG1 to FBG3 caused by temperature rise were obtained. From Fig.2, the maximum temperature measured by FBG4 was about 351°C, and the corresponding temperature sensitivity of the grating should be 9.866pm/°C. Temperature curve changed continuously and stably, which showed the validity and reliability of FBG measurement at high temperature. The thermal stresses at the pasting position of FBG1, FBG2 and FBG3 were get respectively by removing the temperature component from the center wavelength by the Formula (3).As shown in Fig.2, FBG1, FBG2 and FBG3 had a similar thermal stress change characteristics. FBG1 and FBG2 reached the maximum thermal stress of 32299.6 με and 3750.6με at the time of 2190s and 2228s respectively. The time for these two FBGs to reach the maximum thermal strain was roughly the same, with subtle differences owing to the distinct space location and the distance to the heat source. In the measurement process, the signal of FBG2 was discontinuous during a period of time after 1890.7s, and the maximum thermal stress can be measured was only 1819.6με. At the end of the experiment, open the oven, the paste adhesive of FBG2 was found to have been partially burned as a result of the poor paste quality and the fixed tape had been burned. All these may lead to the signal discontinuity of FBG2. Therefore, the quality and reliability of the adhesive paste should be guaranteed during the following experiments.

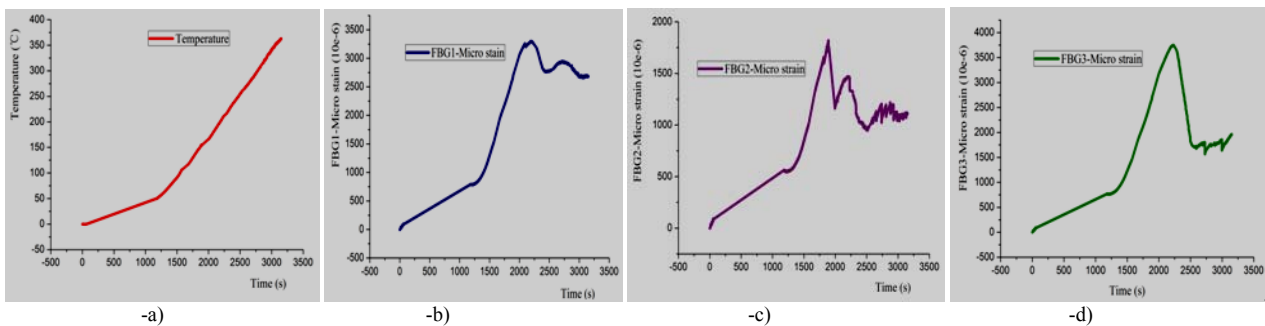


Fig. 2 Temperature and stress distribution of the FBGs.

IV. WELDING STRESS MONITORING OF AN ALUMINUM ALLOY PLATE

A number of branch FBG sensors were attached to the positive surface of a rectangular aluminum alloy plate. This plate and another aluminum plate to be connected with were put together on the welding machine. First, the plate be

connected with and the plate with FBG sensors were compressed by pressure plates in turn, and welded the two plates according to the direction in Fig.3. Waited for 5 minutes after the completion of the welding. Then, Two slots were opened in the welding seam. Welded the slotting parts, and wait another 5 minutes after the secondary welding process. Finally, lifted the pressure plates.

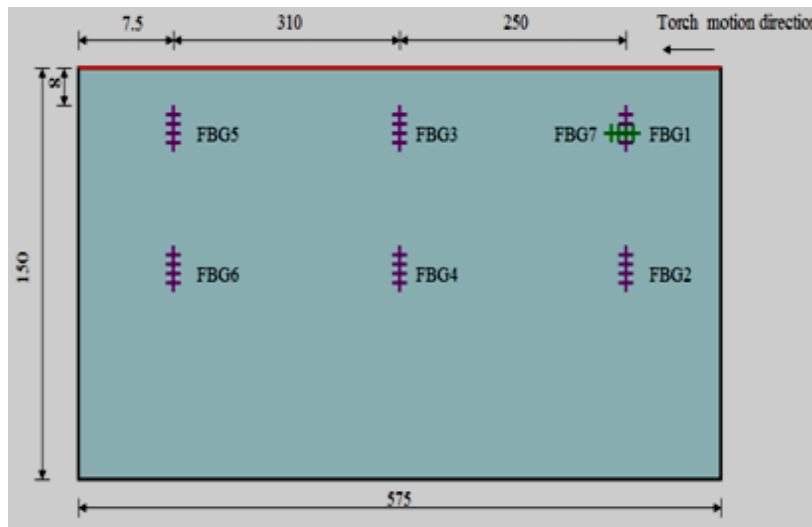


Fig.3. FBGs Layout in the welding stress measurement of the aluminum alloy plate

The maximum change of the center wavelength of the FBG was expected to reach as high as 4-8nm, therefore in order to prevent data aliasing caused by fiber break at high temperature during the welding process and the interference

of the secondary peak as well as the companion mode on the FBG demodulator, it should select FBGs with larger initial wavelength difference and similar reflectivity in the same data channel.

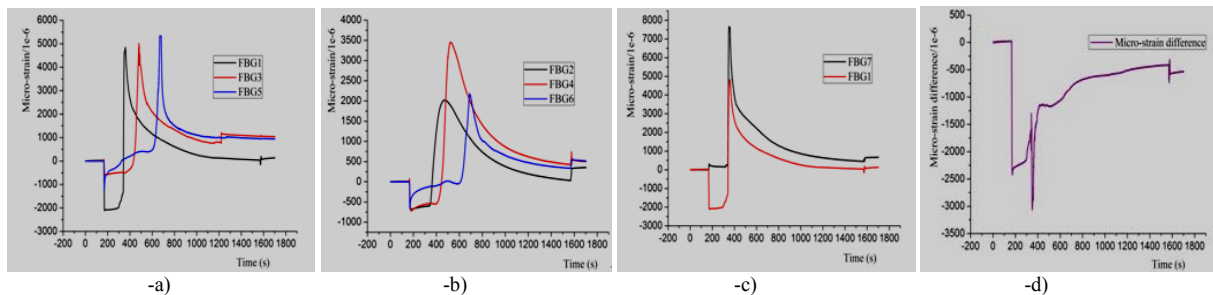


Fig. 4. FBG signals during the first welding process

The FBG paste positions were shown in Fig.3: FBG1 to FBG6 and FBG7 were perpendicular and parallel to the weld seam separately; FBG1, FBG3 and FBG5 were close to the welding seam, while FBG2, FBG4 and FBG6 were located along the same vertical direction of the corresponding FBGs but farer away from the welding seam.

The first welding process started from the right side. The FBG signals during the process were dealt with according to Formula 3, and the results obtained were shown in Fig.4. From Fig.4(a), FBG1, FBG3 and FBG5 had a similar curve distribution characteristic with a sudden change of compressive strain at 170s, which was consistent with the pressing time the aluminum alloy plate. FBG1, FBG3 and FBG5 reached the maximum value of 4807μ ϵ , 5060μ ϵ and 5436μ ϵ successively at the time of 360s, 480s and 677s. The arrival order of the strain peak was in agreement with the welding sequence.

In Fig.4 (b) , there were also strain mutation of FBG2, FBG4 and FBG6 at the time of 170s caused by pressing force. FBG2, FBG4 and FBG6 arrived at the strain peak of 2017μ ϵ , 3452μ ϵ and 2178μ ϵ at the moment of 469s, 524s and 688s sequentially. Their peak arrival times were lower and the peak values were relatively smaller compared with FBG1, FBG3 and FBG5 separately. As FBG2, FBG4 and FBG6 were farer away from the welding seam and there was a certain energy loss through thermal stress conduction, the arrival instant of the maximum stress was somewhat delayed, and the peak value was relatively smaller, which agreed with the actual situation. In Fig.4(c), the strains perpendicular and parallel to the welding direction at the same position were measured by FBG1 and FBG7, respectively. It can be seen from the figure, the strain parallel to the welding direction was greater than that perpendicular to the welding direction at the same

location. The biggest strain difference appeared at about 350s with the value of $3069\mu\epsilon$ in Fig.4(d).

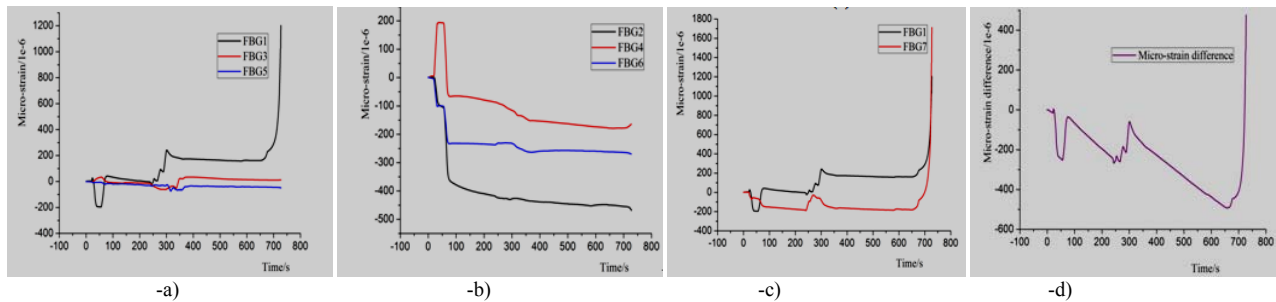


Fig. 5. FBG signals during the second welding process after slotting.

The measurement signals during the second welding process after slotting were shown in Fig.5. As presented in Fig.5, FBG1, FBG3 and FBG5 which were all at the same horizontal line and perpendicular to the welding seam had a similar variation curve, while FBG2, FBG4 and FBG6 had similar curve changing trends with relatively flatter curve and smaller welding strain magnitude. FBG1 which was close to the welded joints was mainly subjected to tensile strain with the maximum value of $246\mu\epsilon$ at the time of 301s, while FBG2 and FBG3 were subjected to smaller compressive strains. FBG4 to FBG6 were mainly affected by the compressive strain, with the maximum value less than $470\mu\epsilon$. Fig.5 (c) showed that the welding stress parallel to the welding direction was tensile stress, while the strain perpendicular to the welding line at the same position was compressive stress, and the difference between them was relatively smaller compared with that in Fig.4. In general, the welding strain range in the second period was smaller than that of the first welding process, which showed that welding stress caused by groove welding was less than that of butt welding.

CONCLUSIONS

A real-time monitoring method for the welding stress of structural parts based on FBG sensing array was studied. Firstly, the reliability and stability of the FBG sensing system were studied. The results showed that the system can measure the temperature and stress field at 350 °C. Based on that, the distributed FBG sensing system was used to monitor the welding strain field of an aluminum alloy plate. The results showed that the sensing FBG response order was in agreement with the welding sequence and the farther away from the weld, the smaller the welding strain was. The welding strain in groove welding process was less than that in butt welding.

ACKNOWLEDGMENTS

This paper is funded and supported by the National Natural Science Foundation of China under Grant

No.51505187 and the New Doctoral Research Projects of Jiangnan University No. 1006-06550001.

REFERENCES

- [1] DIHD Radaj, Heat Effects of Welding, Springer Berlin, 2013.
- [2] Z Zeng, L Wang, P Du, X Li, Determination of welding stress and distortion in discontinuous welding by means of numerical simulation and comparison with experimental measurements, Computational Materials Science.3(2010)535-543.
- [3] DH Won, WS Park, JH Yi, SH Han, TH Han, Effect of welding heat on precast steel composite hollow columns, Structural Concrete,3(2014)350-360
- [4] Jiang D.S., He W, Review of applications for fiber Bragg grating sensors, Journal of Optoelectronics Laser.4(2002)420-430.
- [5] Rodrigo A., Silva-Muñoz, Roberto A., Lopez-Anido, Structural health monitoring of marine composite structural joints using embedded fiber Bragg grating strain sensors, Composite Structures.2(2009)224-234.
- [6] Shimada Yukihiko, Nishimura Akihiko, Development of optical fiber bragg grating sensors for structural health monitoring, Journal of Laser Micro Nanoengineering. 1(2013) 110-114.
- [7] DA Jackson, Recent progress in in-fiber Bragg grating sensors: applications, International Journal of Environmental Studies.2(2007)103-121.